

# Weakly coupled one-dimensional Mott insulators

Fabian H.L. Essler<sup>1</sup> and Alexei M. Tsvelik<sup>2</sup>

<sup>1</sup> *Department of Physics, University of Warwick, Coventry CV4 7AL, UK*

<sup>2</sup> *Department of Physics, Brookhaven National Laboratory, Upton, NY 11973-5000, USA*

We consider a model of one-dimensional Mott insulators coupled by a weak interchain tunnelling  $t_{\perp}$ . We first determine the single-particle Green's function of a single chain by exact field-theoretical methods and then take the tunnelling into account by means of a Random Phase Approximation (RPA). In order to embed this approximation into a well-defined expansion with a small parameter, the Fourier transform  $T_{\perp}(k)$  of the interchain coupling is assumed to have a small support in momentum space such that every integration over transverse wave vector yields a small factor  $\kappa_0^2 \ll 1$ . When  $T_{\perp}(0)$  exceeds a critical value, a small Fermi surface develops in the form of electron and hole pockets. We demonstrate that Luttinger's theorem holds both in the insulating and in the metallic phases. We find that the quasi-particle residue  $Z$  increases very fast through the transition and quickly reaches a value of about 0.4 – 0.6. The metallic state close to the transition retains many features of the one-dimensional system in the form of strong incoherent continua.

PACS numbers: 71.10.Pm, 72.80.Sk

## I. INTRODUCTION

The problem of the Mott metal-insulator transition, which is a consequence of electron interactions and not due to the bandstructure, has been the subject of great interest<sup>1</sup> since the pioneering works by Mott<sup>2</sup>. In 1964 Hubbard suggested a solution of this problem for a particular model<sup>3</sup>. The key point of Hubbard's approach was to take into account the on-site Coulomb interaction  $U$  in zeroth order and develop perturbation theory in  $t/U$ . Unfortunately, the transition from the metallic to the insulating phase is expected to occur when the tunnelling matrix element  $t$  is comparable to the on-site repulsion  $U$ . In this regime expansions in either  $t/U$  or  $U/t$  are not applicable. To overcome this difficulty, various approaches have been suggested. One of them considers a  $SU(N)$ -symmetric generalization of the electronic model and carries out a  $1/N$ -expansion<sup>4,5</sup>. Another approach is based on the so-called Dynamical Mean Field theory, which considers a lattice in infinitely many dimensions  $D \rightarrow \infty$  (see<sup>6</sup> and references therein and also<sup>7,8</sup>).

In this paper we follow a different route. We consider a quasi-one-dimensional model of interacting electrons, where the tunneling along one direction is much larger than in all others. This model can be described in terms of weakly coupled chains. When the band is half-filled and the interchain tunneling is switched off, Umklapp processes dynamically generate a spectral gap  $M$ . The same mechanism can generate gaps at *any* commensurate filling e.g. quarter-filling, but only if the interactions are sufficiently strong. In the half-filled case the decoupled chains develop a Mott-Hubbard gap for any positive value of  $U > 0$ . In what follows we shall assume that the interchain tunneling is weak but *long-ranged*, such that the Fourier transform of the interchain tunneling matrix element has two strong peaks in the Brillouin zone, one around zero wave vector and the other one around  $\mathbf{Q} = (0, \pi, \pi)$  such that

$$T_{\perp}(\mathbf{k}) = -T_{\perp}(\mathbf{k} + \mathbf{Q}) \quad (1)$$

Due to the long-range character of the tunneling, the width of these peaks, denoted by  $\kappa_0$ , is small ( $\kappa_0 \ll 1$ ). Hence every integration over the transverse momentum yields a small parameter  $\kappa_0^2$ . The main idea of our approach is to treat the individual chains non-perturbatively and then to employ the Random Phase Approximation (RPA) to take into account the interchain tunneling. Since the Mott metal-insulator transition is associated with development of a coherent single-particle excitation branch, the correlation function we are interested in is the single-electron Green's function  $G$ . The RPA expression for  $G$  is

$$G(\omega, q, \mathbf{k}) = [G_0^{-1}(\omega, q) - T_{\perp}(\mathbf{k})]^{-1}, \quad (2)$$

where  $q$  is the momentum along the chain direction and  $G_0$  is the single-particle Green's function for an individual chain. The corrections to RPA are of higher order in  $\kappa_0^2$ , which is the small parameter in our expansion. The smallness of  $\kappa_0^2$  suppresses multiparticle tunneling processes, which generate exchange interactions between the chains and eventually lead to a three-dimensional phase transition. However, for small  $\kappa_0^2$  the temperature at which this transition occurs is much smaller than the characteristic energy scale  $M$  of the problem. Therefore throughout the paper we shall assume that we work at temperatures much smaller than  $M$  (such that the thermal effects on the single-particle Green's function can be neglected) but much larger than the transition temperature  $T_c$ , i.e.  $T_c \ll T \ll M$ . We note that an analogous RPA has been used by Wen<sup>9</sup> to study weakly coupled Luttinger liquids (LL), see also<sup>10</sup> for a derivation based on functional integrals. An improved calculation for the case of coupled LLs has recently been carried out by Arrighi<sup>11</sup>. It is based on taking into account multipoint correlation functions of upcoupled chains in a controlled way. In a Mott insulator multipoint correlation functions are much more difficult to determine than in a LL. We

therefore postpone the discussion of corrections to RPA until future publications.

We also neglect the long distance tails of the Coulomb interaction. This can be justified at finite temperatures if the dielectric constant at small frequencies is large.

The basic input of our approach is  $G_0$ . To calculate this function we assume that for an isolated chain the Mott-Hubbard gap  $M$  is much smaller than the band width  $D_{\parallel}$ . In this case one can use the continuous field theoretical description in the low energy limit. The corresponding field theory will be described in detail in the next section and is highly universal; all information about the underlying lattice model is incorporated in just three dimensionless constants. Thus, our assumptions can be summarized by the inequalities

$$\begin{aligned} D_{\parallel} &\gg M(U) \approx t_{\perp}(0) \gg t_{\perp}(|k| > \kappa_0), \\ T_c &\ll T \ll M \end{aligned} \quad (3)$$

where  $(U)$  symbolizes dependence of the Mott-Hubbard gap from the interactions. The smallness of  $M$  does not imply that the interactions are weak. For example, in the Hubbard model the field theoretical description works well even for  $U/t_{\parallel}$  as large as 2-3 (see, for example,<sup>12</sup>). At such interaction strength one should expect the spin and charge velocities to be considerably different. This is a consequence of spin-charge separation, which is one of the most interesting features of one-dimensional strongly correlated systems. The effects of spin-charge separation in the insulating regime deserve a special discussion, which will be given later in the paper.

The outline of this paper is as follows. In section II we introduce the model and discuss the limit of decoupled chains. In section VI we take the interchain coupling into account and determine various physics properties.

In section VII we discuss possible experimental applications.

## II. THE MODEL

We take as a starting point the following lattice model of correlated electrons

$$\begin{aligned} H &= \sum_l H^{(l)} + \sum_{l,m,n,\sigma} t_{lm} c_{n,\sigma}^{(l)\dagger} c_{n,\sigma}^{(m)} + \text{h.c.} \\ H^{(l)} &= -t \sum_{n,\sigma} c_{n,\sigma}^{(l)\dagger} c_{n+1,\sigma}^{(l)} + \text{h.c.} + U \sum_n n_{j,\uparrow}^{(l)} n_{j,\downarrow}^{(l)}. \end{aligned} \quad (4)$$

Here  $l, m$  label Hubbard chains and  $n$  labels the sites along a given chain. In the physically most interesting situation the interchain hopping matrix elements  $t_{lm}$  are taken to be equal to  $t_{\perp}$  if  $l$  and  $m$  are nearest neighbours and zero otherwise. For this choice of interchain hopping our calculational scheme is uncontrolled: there is no small expansion parameter. One may nevertheless apply our scheme and hope that the corrections are small in some regime of temperatures. On the other hand one may

choose the  $t_{nm}$ 's in such a way that a small expansion parameter is introduced, as explained above and in more detail in Appendix A.

Let us first consider the case of uncoupled chains  $t_{\perp} = 0$ . For weak repulsion  $U < t$  and low energies a field-theory description is appropriate. Keeping only modes in the vicinity of the Fermi momenta  $\pm k_F = \pm \pi/2a_0$ , we may decompose the lattice Fermi operators as

$$c_{n,\sigma}^{(l)} = \sqrt{a_0} \left[ \exp(ik_F x) R_{\sigma}^{(l)}(x) + \exp(-ik_F x) L_{\sigma}^{(l)}(x) \right], \quad (5)$$

where  $a_0$  is the lattice spacing. Inserting this prescription into the Hamiltonian (4) and dropping the chain index  $(l)$  for the time being, one obtains

$$\begin{aligned} \mathcal{H} &= \sum_{\sigma} v_F \int dx \left[ L_{\sigma}^{\dagger} i \partial_x L_{\sigma} - R_{\sigma}^{\dagger} i \partial_x R_{\sigma} \right] \\ &+ \frac{g}{3} \int dx \left[ : \mathbf{I} \cdot \mathbf{I} : + : \bar{\mathbf{I}} \cdot \bar{\mathbf{I}} : - : \mathbf{J} \cdot \mathbf{J} : - : \bar{\mathbf{J}} \cdot \bar{\mathbf{J}} : \right] \\ &+ 2g \int dx \left[ \mathbf{I} \cdot \bar{\mathbf{I}} - \mathbf{J} \cdot \bar{\mathbf{J}} \right]. \end{aligned} \quad (6)$$

where  $v_F = 2ta_0$  is the Fermi velocity and  $g = Ua_0$ . Here  $\mathbf{J}$  and  $\mathbf{I}$  are the chiral components of SU(2) spin and pseudospin currents

$$\begin{aligned} I^3 &= \frac{1}{2} \sum_{\sigma} : L_{\sigma}^{\dagger} L_{\sigma} : , \quad I^{+} = L_{\uparrow}^{\dagger} L_{\downarrow}^{\dagger} , \\ \bar{I}^3 &= \frac{1}{2} \sum_{\sigma} : R_{\sigma}^{\dagger} R_{\sigma} : , \quad \bar{I}^{+} = R_{\uparrow}^{\dagger} R_{\downarrow}^{\dagger} , \\ J^3 &= \frac{1}{2} \left( L_{\uparrow}^{\dagger} L_{\uparrow} - L_{\downarrow}^{\dagger} L_{\downarrow} \right) , \quad J^{+} = L_{\uparrow}^{\dagger} L_{\downarrow} , \\ \bar{J}^3 &= \frac{1}{2} \left( R_{\uparrow}^{\dagger} R_{\uparrow} - R_{\downarrow}^{\dagger} R_{\downarrow} \right) , \quad \bar{J}^{+} = R_{\uparrow}^{\dagger} R_{\downarrow} . \end{aligned} \quad (7)$$

By employing the Sugawara construction, the Hamiltonian (6) can now be split into two parts, corresponding to the spin and charge sectors respectively<sup>13</sup>

$$\begin{aligned} \mathcal{H} &= \mathcal{H}_c + \mathcal{H}_s , \\ \mathcal{H}_s &= \frac{2\pi v_s}{3} \int dx \left[ : \mathbf{J} \cdot \mathbf{J} : + : \bar{\mathbf{J}} \cdot \bar{\mathbf{J}} : \right] - 2g \int dx \mathbf{J} \cdot \bar{\mathbf{J}} , \\ \mathcal{H}_c &= \frac{2\pi v_c}{3} \int dx \left[ : \mathbf{I} \cdot \mathbf{I} : + : \bar{\mathbf{I}} \cdot \bar{\mathbf{I}} : \right] + 2g \int dx \mathbf{I} \cdot \bar{\mathbf{I}} . \end{aligned} \quad (8)$$

Here  $v_s = v_F - Ua_0/2\pi$  and  $v_c = v_F + Ua_0/2\pi$ . Apart from the (marginally) irrelevant current-current interaction in the spin sector and the difference in spin and charge velocities, the Hamiltonian (8) is identical to the one of the SU(2) Thirring model. The SU(2) Thirring model can be bosonized in terms of a Sine-Gordon model and a free boson; the resulting action density is

$$\begin{aligned} \mathcal{S}_s &= \frac{1}{16\pi} \left[ v_s^{-1} (\partial_{\tau} \Phi_s)^2 + v_s (\partial_x \Phi_s)^2 \right] , \\ \mathcal{S}_c &= \frac{1}{16\pi} \left[ v_c^{-1} (\partial_{\tau} \Phi_c)^2 + v_c (\partial_x \Phi_s)^2 \right] + \lambda \cos(\beta \Phi_c) , \end{aligned} \quad (9)$$

where  $\beta = 1$ . If we consider additional small density-density interactions between nearest neighbour sites in (4) the field theory limit is again of the form (9), but now  $\beta < 1$ . Using the integrability of the model (9) it is possible to determine dynamical correlation functions. This is the subject of the following section.

### III. UNCOUPLED CHAINS

The calculation of the spectral function for half-filled Mott insulators is based on the following principles:

(a) Locality:  $R_\alpha, L_\alpha$  are local fields. This allows us to employ the standard formfactor approach<sup>14</sup>. Some important elements of this approach are reviewed in Appendix B.

(b) Spin-Charge separation: The Hamiltonian (8) is the sum of two parts representing the spin and charge degrees of freedom respectively and by means of bosonization one can represent  $R_\alpha, L_\alpha$  as products of fields belonging to the different sectors. For example:

$$R_\sigma = \frac{\eta_\sigma}{2\pi} \exp\left(\frac{i}{2}\phi_c\right) \exp\left(\pm\frac{i}{2}\phi_s\right), \quad (10)$$

where  $\phi_c, \phi_s$  are chiral components of the bosonic fields,  $\eta_\sigma$  are Klein factors and the plus (minus) sign corresponds to  $\sigma = \uparrow$  ( $\sigma = \downarrow$ ). The components into which the creation and annihilation operators are factorized are nonlocal fields, but the factorization of the field means that all its formfactors also factorize, at least in the limit when one of the sectors becomes massless.

(c) “Triviality” of the spin sector: In the limit  $g_s \rightarrow 0$  the field theory for the spin sector becomes massless and the correlation function of the spin exponent in (10) is simply given by

$$\left\langle \exp\left[\frac{i}{2}\phi_s(x, \tau)\right] \exp\left[-\frac{i}{2}\phi_s(0)\right] \right\rangle = \frac{1}{\sqrt{v_s\tau - ix}}. \quad (11)$$

(d) Lorentz invariance and Watson’s theorem: Let us consider formfactors of the left moving fermi operator  $L_\sigma(x)$ . The first nonvanishing formfactor is between the vacuum and a scattering state of one spinon (with spin  $\sigma$ ) and one antiholon. We denote the rapidity of the spinon (antiholon) by  $\theta_s$  ( $\theta_c$ ) (our notations are summarised in Appendix B). Lorentz invariance and Watson’s theorem impose the following form for the first nonvanishing formfactor for the fermion operator

$$\langle 0|L_\sigma(0)|\theta_c, \theta_s\rangle_{\bar{h}s} = \exp[(\theta_c + \theta_s)/4] f(\theta_c - \theta_s). \quad (12)$$

The function  $f(\theta)$  is periodic with period  $2i\pi$  and does not contain poles. Furthermore the usual asymptotic bound<sup>16</sup> yields

$$\lim_{\alpha \rightarrow \infty} \langle 0|L|\theta_c, \theta_s\rangle \exp\left(-\frac{\theta_\alpha}{4}\right) \leq \text{const}, \quad (13)$$

where  $\alpha = c, s$ . This leaves us with the only possibility  $f(\theta) = \text{const}$ . As we see, this matrix element does not depend on the anisotropy of the interaction (up to a constant prefactor). The reason for this is that all information about the anisotropy of the coupling constants is contained in the two-particle S-matrices of holons and spinons and does not influence the single-particle emission. An explicit expression for  $f$  has recently been obtained in<sup>15</sup>; for  $\beta^2 \rightarrow 1$  (the isotropic case) the numerical value is

$$f = (Z_0/2\pi)^{1/2}; \quad Z_0 = 0.9218. \quad (14)$$

The matrix element (12) describes the emission of one kink in the charge and one kink in the spin sector. The charge part of this first term in the expansion is thus equal (up to a overall numerical factor) to

$$\begin{aligned} & \int_{-\infty}^{\infty} d\theta e^{\theta/2} \exp[-m\tau \cosh \theta - im\frac{x}{v_c} \sinh \theta] \\ &= \left(\frac{\tau v_c - ix}{\tau v_c + ix}\right)^{\frac{1}{4}} K_{\frac{1}{2}}(m\sqrt{\tau^2 + x^2 v_c^{-2}}) \\ &= \frac{\exp[-m\sqrt{\tau^2 + x^2 v_c^{-2}}]}{\sqrt{v_c\tau + ix}} \end{aligned} \quad (15)$$

In the next step we use the fact that the single-electron Green’s function factorizes into a charge and a spin piece. Let us consider intermediate states containing a single antiholon and any number of spinons. Factorization implies that if we carry out the sum over all multi-spinon contributions, we must obtain the conformal result (11) for the spin sector. Therefore we arrive at the following result for the two-point function

$$\langle L_\sigma(x, \tau) L_\sigma^\dagger(0, 0) \rangle \simeq \frac{Z_0}{2\pi} \frac{\exp[-m\sqrt{\tau^2 + x^2 v_c^{-2}}]}{\sqrt{(v_s\tau + ix)(v_c\tau + ix)}}, \quad (16)$$

The leading corrections to (16) involve intermediate states containing two antiholons and one holon and are thus of order  $\mathcal{O}(\exp(-3mr))$ . Similarly we have

$$\langle R_\sigma(x, \tau) R_\sigma^\dagger(0, 0) \rangle \simeq \frac{Z_0}{2\pi} \frac{\exp[-m\sqrt{\tau^2 + x^2 v_c^{-2}}]}{\sqrt{(v_s\tau - ix)(v_c\tau - ix)}}. \quad (17)$$

Eqns(16-17) were first written down by Wiegmann (for  $v_c = v_s$ )<sup>17</sup>. This remarkable result appears to have been subsequently forgotten and rediscovered only much later by Voit, who conjectured the same form the Green’s function<sup>18</sup>. The correct form was again reproduced by Sarykh *et al.*<sup>19</sup>, although on the basis of arguments which cannot be accepted as rigorous. An earlier attempt to calculate the single particle Green’s function using the formfactor approach<sup>20</sup> led to an incorrect result yielding  $K_1$ -function instead of  $K_{\frac{1}{2}}$  in Eq.(15). Finally, Parola and Sorella<sup>21</sup> determined the spectral function by mapping the problem of a single hole in a Mott insulator

onto an effective spin chain with skew boundary conditions. Their results are somewhat implicit so that it is difficult to compare them to (17).

To conclude this section we would like to remark that the above results can be generalized to the case of the  $SU(N)$  Thirring model

$$\langle L_\sigma(x, \tau) L_\sigma^\dagger(0, 0) \rangle = \frac{Z_0(N)}{2\pi} \frac{1}{(v_s \tau + ix)^{\frac{1}{N}}} \times \left( \frac{v_c \tau - ix}{v_c \tau + ix} \right)^{\frac{1}{2} - \frac{1}{2N}} K_{1-\frac{1}{N}}(m \sqrt{\tau^2 + x^2 v_c^{-2}}). \quad (18)$$

Here we have used that the kinks in the  $SU(N)$  Thirring model have spin  $\frac{1}{2}(1 - \frac{1}{N})^{22}$ . A similar formula with  $x \rightarrow -x$  holds for the right-moving fermions.

### A. Short-distance behaviour: RG calculations.

Strictly speaking, single kink emissions in the charge sector allow one to consider only the frequencies up to  $3m$  which is the threshold for the emission of two antiholons and one holon. However, since the numerical value of  $Z_0$  is quite close to one eqns (16,17) are likely to provide a very good description of the Green's function in the entire frequency interval. Indeed, considering the short-distance (high energy) behaviour ( $m \sqrt{\tau^2 + x^2 v_c^{-2}} \ll 1$ ) in (17) and (16) we recover the standard expressions for the Green's functions of the Luttinger liquid (modulo the prefactor  $Z_0$ , which, as we have said, is almost 1). A better description of the short-distance behaviour is obtained by carrying out a renormalisation group (RG) analysis. The RG equations for the coupling constant  $g$  and wave function renormalisation  $Z$  in the case  $v_c = v_s = v$  are

$$g_0 = g + \frac{g^2}{2\pi} \ln \frac{\Lambda^2}{\mu^2} + \mathcal{O}(g^3), \quad (19)$$

$$Z = 1 - \frac{3}{32\pi^2} g^2 \ln \frac{\Lambda^2}{\mu^2} + \mathcal{O}(g^3), \quad (20)$$

where  $\Lambda$  is a UV cutoff and  $\mu$  a subtraction point. The RG improved result for the two-point function is thus

$$\langle R_\sigma(x, \tau) R_\sigma^\dagger(0, 0) \rangle = \frac{Z(r)}{2\pi(v\tau - ix)}, \quad (21)$$

where

$$Z(r) \simeq 1 - \frac{3}{16\pi} g(r), \quad g(r) \simeq -\frac{\pi}{\ln(rm)}, \quad r^2 = x^2 + v^2 \tau^2 \ll m^{-2}. \quad (22)$$

Comparing this to (17) for short distances, we find very good agreement. In the anisotropic case, where the short-distance behaviour of the Green's function is controlled by the Luttinger liquid exponent, the agreement becomes

worse. For “large” anisotropy it may become necessary to take intermediate states with e.g. two solitons and one antisoliton into account in order to get a good description of the Green's function over a large range of energies.

### B. Retarded dynamical Green's function

Given the expression (17) for the Green's function in position space we can calculate the dynamical Green's function by Fourier transformation and subsequent analytic continuation to real frequencies. A straightforward calculation gives the following result for the retarded Green's function

$$G_{RR}^{(R)}(\omega, q) = -Z_0 \sqrt{\frac{2}{1+\alpha}} \frac{\omega + v_c q}{\sqrt{m^2 + v_c^2 q^2 - \omega^2}} \times \left[ \left( m + \sqrt{m^2 + v_c^2 q^2 - \omega^2} \right)^2 - \frac{1-\alpha}{1+\alpha} (\omega + v_c q)^2 \right]^{-\frac{1}{2}} \quad (23)$$

where  $\alpha = v_s/v_c$ . At  $\alpha = 1$  this simplifies to

$$G_{RR}^{(R)}(\omega, q) = -\frac{Z_0}{\omega - vq} \left[ \frac{m}{\sqrt{m^2 + v^2 q^2 - \omega^2}} - 1 \right]. \quad (24)$$

### C. Spectral function

The spectral function is defined as

$$A_{RR}(\omega, q) = -\frac{1}{\pi} \text{Im} G_{RR}^{(R)}(\omega, q). \quad (25)$$

In the limit  $v_c = v_s = v$  we obtain from (24) the following simple result

$$A_{RR}(\omega, q) = \frac{Z_0 m}{\pi |\omega - vq|} \frac{\Theta(|\omega| - \sqrt{m^2 + v^2 q^2})}{\sqrt{\omega^2 - m^2 - v^2 q^2}}. \quad (26)$$

An explicit expression for the general case  $v_s \neq v_c$  is easily obtained from (23). We note that the result is exact for energies  $\omega \leq 3m$  as the intermediate states involving more than one antiholon will start contributing only at this energy. However, from previous experience<sup>39</sup> as well as on the basis of the arguments given above, we expect (23) to be an excellent approximation up to very high energies.

For general  $v_c, v_s$  the spectral function is nonvanishing in a region with boundary  $\omega = \epsilon(p)$  defined by the equation

$$\epsilon(p) = \min_q [v_s |p - q| + \sqrt{v_c^2 q^2 + m^2}]. \quad (27)$$

The solution of this equation is

$$\epsilon(p) = \begin{cases} \sqrt{m^2 + v_c^2 p^2} \equiv \epsilon_0(p) & \text{if } p \leq Q \\ v_s p + m\sqrt{1 - \alpha^2} \equiv \epsilon_1(p) & \text{if } p \geq Q \end{cases}, \quad (28)$$

where

$$Q = \frac{mv_s}{\sqrt{1 - (v_s/v_c)^2}}. \quad (29)$$

The spectral function generally has several kinds of singularities. Firstly, there are singularities just above the threshold. For small momenta  $|q| \ll Q$  there is a square root singularity above the threshold  $\omega = \epsilon(q)$

$$A(\omega, q) \simeq \frac{Z_0}{\pi} \frac{\epsilon_0(q) + v_c q}{\sqrt{2\epsilon_0(q)}} ([q + \epsilon_0(q)][\alpha\epsilon_0(q) - q])^{-\frac{1}{2}} \times \frac{1}{\sqrt{\omega - \epsilon_0(q)}}. \quad (30)$$

There also is a square root singularity above the threshold for “large” momenta  $|q| \gg Q$ , where

$$A(\omega, q) \simeq \frac{Z_0}{\pi\sqrt{v_c - v_s}} \frac{1}{\sqrt{|q| - Q}} \frac{1}{\sqrt{\omega - \epsilon_1(q)}}. \quad (31)$$

This square root singularity is a general feature of the half-filled Mott insulator and apparently holds for any ratio of the gap to the bandwidth. Calculations done for a model where this ratio is infinite<sup>23</sup> gave the same singularity.

In addition there is a second square-root singularity for  $\omega \rightarrow \epsilon_0(q)$  from below

$$A(\omega, q) \simeq \frac{Z_0}{\pi} \frac{\epsilon_0(q) + v_c q}{\sqrt{2\epsilon_0(q)}} ([q + \epsilon_0(q)][v_c q - \alpha\epsilon_0(q)])^{-\frac{1}{2}} \times \frac{1}{\sqrt{\epsilon_0(q) - \omega}}. \quad (32)$$

For  $q = Q$  these two singularities collapse onto a single one and we have

$$A(\omega, Q) \simeq \frac{Z_0}{\pi} \left( \frac{1 + \alpha}{1 - \alpha} \right)^{\frac{1}{4}} 2^{-\frac{5}{4}} \epsilon(Q)^{-\frac{1}{4}} (\omega - \epsilon(Q))^{-\frac{3}{4}}. \quad (33)$$

In Fig.1 we show the spectral function for  $v_c = v_s = v$  as a function of  $\omega$  and  $q$ . As  $Q = \infty$  in this case the threshold is simply given by  $\omega = \sqrt{m^2 + v^2 q^2}$ . The square root singularities above the threshold are visible as regions of high spectral weight.

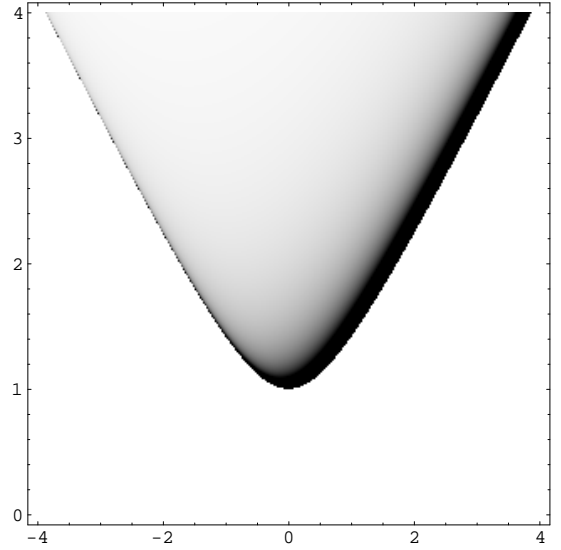


FIG. 1. Density plot of the spectral function  $A_{RR}(\omega, q)$  as a function of  $\omega$  and  $vq/m$  for  $v_s = v_c = v$ .

Fig.2 shows a constant energy scan at  $\omega = 3m$ .

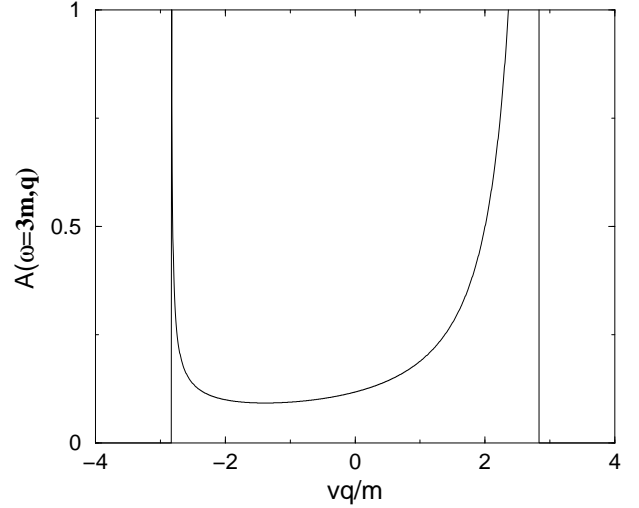


FIG. 2. Constant energy ( $\omega = 3m$ ) scan of the spectral function for  $\alpha = 1$ .

When we allow the spin and charge velocities to be different an interesting effect occurs as can be seen from the density plot of  $A_{RR}(\omega, q)$  in Fig.3. For momenta  $q < Q$  the threshold occurs at the gap for a single soliton moving with momentum  $q$  and the spectral function looks very much like it did in the case  $\alpha = 1$ . However, at momenta  $q > Q$  the threshold gets shifted to  $\omega = v_s q + m\sqrt{1 - \alpha^2}$  and a lot of spectral weight is concentrated between this threshold and the line  $\omega = \sqrt{m^2 + v_c^2 q^2}$ , where a second singularity occurs (see above). This is shown in the constant energy scan Fig.4. For large momenta  $v_{s,c}q \gg m$  the double singularity at  $\omega \simeq v_{c,s}q$  is similar to what occurs in a Luttinger liquid<sup>24</sup>.

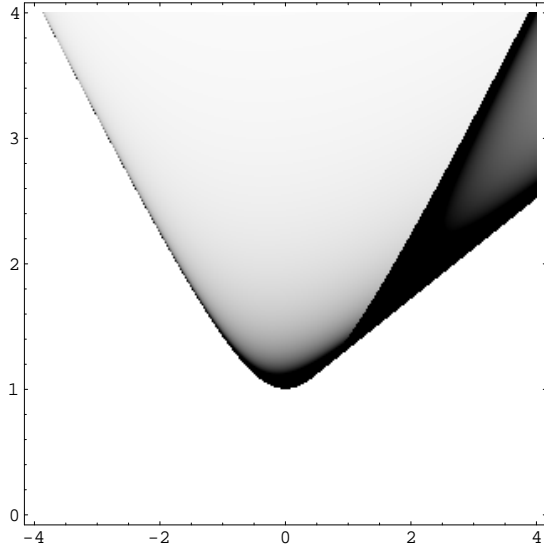


FIG. 3. Density plot of the spectral function  $A_{RR}(\omega, q)$  as a function of  $\omega$  and  $v_c q/m$  for  $\alpha = 0.4$ .

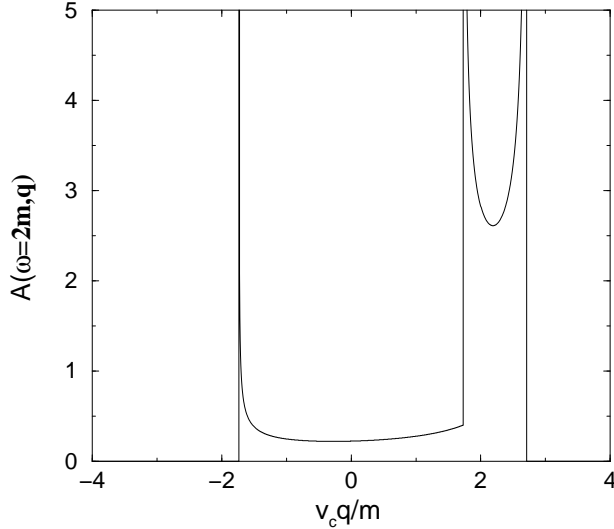


FIG. 4. Constant energy ( $\omega = 2m$ ) scan of the spectral function for  $\alpha = 0.4$ .

The states located in the “wedge”  $\epsilon_1(q) < \omega < \epsilon_0(q)$  correspond to a situation where the single antiholon carries only a small part of the total momentum and the remainder is made up by exciting (many) spinons. This effect is reminiscent of Cherenkov radiation produced by a heavy particle moving through a medium with a speed greater than the speed of light in this medium.

#### D. Tunneling density of states

From the Matsubara Green’s function at coinciding space points in model (8) we extract the single-particle density of states

$$\rho(\omega) = -2\text{Im } G^{(R)}(\omega, x=0) = \frac{2Z_0}{v_s v_c} \theta(|\omega| - m). \quad (34)$$

The density of states (34) is *constant* for energies higher than the single-particle gap  $m$ . Formula (34) is exact for  $|\omega| \leq 3m$  and expected to be an excellent approximation up to very high energies.

#### IV. COHERENT SINGLE-PARTICLE MODE GENERATED BY THE INTERCHAIN TUNNELLING

Taking the interchain tunneling into account in the RPA yields an expression for the single-electron function in the form of (2). The interchain tunneling gives rise to a branch of coherent excitations below the threshold of the 1D spectral function  $A(\omega, q)$  in the region where  $T_\perp(\vec{k}) < 0$ . Therefore, even an infinitesimal interchain coupling leads to the coherent particle motion in the transverse direction and there is no confinement in the sense of Anderson<sup>25</sup>.

##### A. $v_s = v_c$

Let us first discuss the case  $v_s = v_c = v$ . For very small interchain tunnelling  $|T_\perp(\vec{k})| \ll m$  the pole of (2) appears at a finite frequency very close to  $\epsilon_0(p) = \sqrt{p^2 + m^2}$ . In the vicinity of the pole we have

$$G(\omega, q, \vec{k}) \approx \frac{Z(q, \vec{k})}{\omega - \epsilon(q, \vec{k})}, \quad (35)$$

where  $Z(q, \vec{k})$  varies strongly at small  $q$  and where for  $|vq| \ll |m^2/Z_0 T_\perp(\vec{k})|$

$$\epsilon(q, \vec{k}) = \epsilon_0(q) - \left( \frac{Z_0 T_\perp(\vec{k}) m}{\sqrt{2\epsilon_0(q)} [\epsilon_0(q) - vq]} \right)^2. \quad (36)$$

In the chain direction, the dispersion of the coherent mode is asymmetric around  $q = 0$  and has a minimum at  $vq \simeq [Z_0 T_\perp(\vec{k})]^2/m$ . For larger values of  $T_\perp(\vec{k})$  this picture remains qualitatively unchanged although the dispersion law becomes more complicated. In the vicinity of the minimum the dispersion is approximately given by

$$\epsilon(q, \vec{k}) \approx \sqrt{\omega_0^2 + v^2(q - q_0)^2}, \quad (37)$$

where  $\omega_0, q_0$  depend only on  $T_\perp(\vec{k})$ . At large positive  $vq \gg m$  we have

$$\epsilon(q, \vec{k}) \approx vq + Z_0 T_\perp(\vec{k}), \quad (38)$$

and at large negative  $vq \ll -\max(m, |Z_0 T_\perp(\vec{k})|)$

$$\epsilon(q, \vec{k}) \approx \sqrt{m^2 + (vq)^2 - \left[ \frac{Z_0 T_\perp(\vec{k})}{2vq} \right]^2}. \quad (39)$$

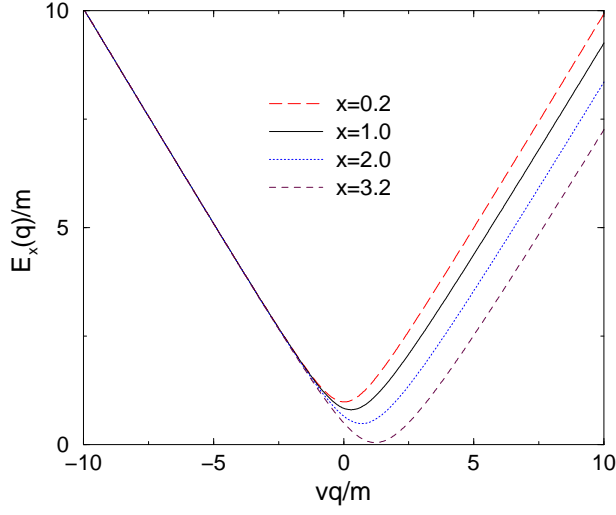


FIG. 5. Dispersion of the coherent mode along the chain direction for several values of  $x = -Z_0 T_\perp(\vec{k})$  and  $\alpha = 1$ .

The dispersion of the coherent mode depends on the transverse momentum only through  $T_\perp(\vec{k})$ . In Fig.5 we plot

$$E_x(q) \equiv \epsilon(q, \vec{k}) \Big|_{-Z_0 T_\perp(\vec{k})=x} \quad (40)$$

as a function of  $q$  for several values of  $x$ . In Fig. 6 we plot the residue of the coherent mode for various  $x$  versus  $qv/m$ .

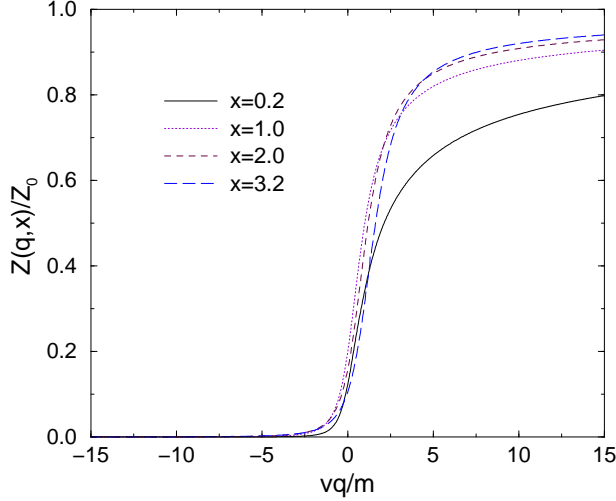


FIG. 6. Residue of the coherent mode as a function of the momentum along the chain direction for several values of  $x = -Z_0 T_\perp(\vec{k})$  and  $\alpha = 1$ .

We see that  $Z(q, \vec{k})$  is very small within the noninteracting Fermi surface.

## B. $v_s \neq v_c$

The case of different velocities can be dealt with in a completely analogous way. In Fig.7 we show the spectral function as a function of energy and momentum transfer along the chain direction for weak tunnelling  $Z_0 T_\perp(\vec{k}) = 0.5$ . The coherent mode is clearly visible below the threshold of the one dimensional spectral function.

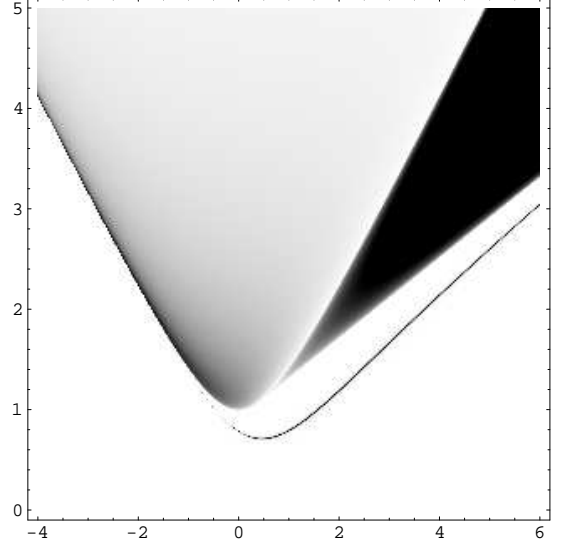


FIG. 7. Density plot of the spectral function  $A_{RR}(\omega, q, \vec{k})$  as a function of  $\omega$  and momentum transfer along the chain direction  $q$  for  $Z_0 T_\perp(\vec{k}) = 0.5$ .

In Fig.8 we show a constant energy scan of the spectral function.

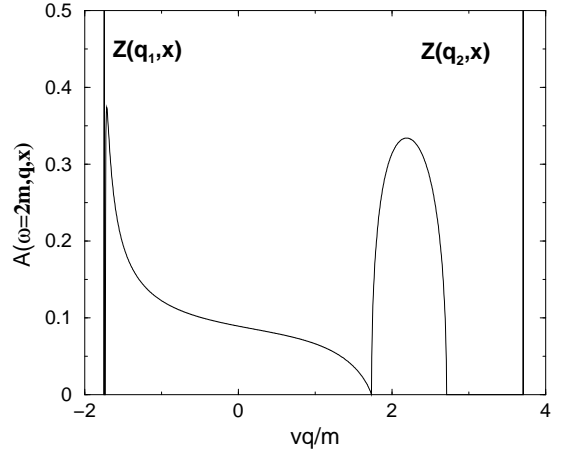


FIG. 8.  $A_{RR}(\omega, q, \vec{k})$  as a function of the momentum along the chain direction for  $\omega = 2m$ ,  $\alpha = 0.4$  and  $Z_0 T_\perp(\vec{k}) = 0.5$ .

If we compare Fig.8 to the corresponding plot of the spectral function of uncoupled chains in Fig.4, we notice

that now there are two delta function peaks corresponding to the coherent mode, and that the singularities of the incoherent scattering continuum have been smoothed out. It turns out that most ( $\simeq 75\%$ ) of the spectral weight for fixed  $T_\perp(\mathbf{k})$  (i.e. we integrate only over  $q$ ) is located in the coherent mode at  $q_2$ , about 23% sits in the incoherent spinon-antiholon continuum and only 2% is due to the coherent branch at  $q_1$ . The sharp difference between the weights in the coherent modes is consistent with the picture presented on Fig. 6.

As  $t_\perp$  increases more and more of the spectral weight gets transferred to the coherent mode. For example, for  $Z_0 T_\perp(\tilde{k}) = 3.2m$  approximately 95% of the spectral weight at energy  $\omega = 2m$  is located in the coherent mode at  $q_2$ . However, it is important to note that the coherent modes dominate only a small portion of the Brillouin zone (the part where  $T_\perp(\mathbf{k})$  is large). If we consider the total spectral weight, i.e. integrate over the transverse momentum  $\mathbf{k}$  as well, we find that the contribution of the coherent mode is generally small.

## V. FERMI SURFACE AND LUTTINGER'S THEOREM

According to Luttinger's theorem the total number of particles in the system is proportional to the volume of momentum space included in the surface defined by the singularities of  $\ln G(\omega = 0, \mathbf{p})$ . These singularities may be due to either poles or zeroes of the single-particle Green's function. As was recently emphasized by Dzyaloshinskii<sup>26</sup>, the latter possibility must occur in Mott insulators thus removing an apparent violation of Luttinger's theorem by the interactions. Indeed the Green's function (23) exhibits precisely this property: at  $\omega = 0$  it vanishes at  $q = 0$ , which corresponds to the Fermi surface of the non-interacting system. Since the position of the zeroes is unchanged in RPA, our results are in agreement with Luttinger's theorem.

When  $t_\perp$  exceeds a critical value, electron- and hole-like pockets of Fermi surface appear. The Fermi surface is determined by the equation

$$G_0^{-1}(0, q) = T_\perp(\mathbf{k}) \quad (41)$$

The volumes of electron and hole pockets are equal since  $T_\perp(\mathbf{k}) = -T_\perp(\mathbf{Q} + \mathbf{k})$  where  $\mathbf{Q} = (\pi, \pi, 0)$ . So Luttinger's theorem continues to hold.

Using the fact that at  $\omega = 0$  the Green's function is always real, we get from (23)

$$\begin{aligned} [Z_0 T_\perp(\mathbf{k})]^2 &= \frac{(v_c^2 q^2 + m^2)(m + \alpha \sqrt{v_c^2 q^2 + m^2})}{\sqrt{v_c^2 q^2 + m^2} - m}, \\ \text{sign}(T_\perp(\mathbf{k})) &= -\text{sign}(q). \end{aligned} \quad (42)$$

The critical value of  $T_\perp(\mathbf{k})$  necessary to produce the solution is

$$\left[ \frac{Z_0 t_\perp^{\min}}{m} \right]^2 = 3 + \frac{9\alpha + 1}{2} x_0, \quad (43)$$

where  $x_0$  is determined by the momentum  $q_0$  where the Fermi surface first appears

$$x_0 = \sqrt{1 + v_c^2 q_0^2 / m^2} = \frac{3\alpha - 1 + \sqrt{1 + 10\alpha + 9\alpha^2}}{4\alpha}. \quad (44)$$

The critical value of  $Z_0 t_\perp^{\min}$  varies from  $2m$  at small  $v_s$  to  $\sim 3.3m$  for  $v_s = v_c$ .

The residue at the Fermi surface is given by

$$Z = \frac{2Z_0}{(1 + \alpha)} \frac{(x - 1)}{x} \left[ \frac{(x\alpha + 1)}{(x + 1)} \right]^{1/2}, \quad (45)$$

where  $x \equiv \sqrt{1 + v_c^2 q^2 / m^2}$ . Near the critical value of  $T_\perp(\mathbf{k})$  the residue is numerically small but never goes to zero. For example, in the limit  $v_s \rightarrow 0$  when  $x = 2$  we get

$$Z(v_s \rightarrow 0) \approx 0.58 Z_0$$

and at  $v_s = v_c$  when  $x \approx 1.62$  we have

$$Z(v_s = v_c) \approx 0.38 Z_0.$$

For a cubic lattice the Fermi surface forms an *electron pocket* around  $\tilde{q} = q_0 > 0$ ,  $k_0^y = k_0^z = 0$  and *hole pockets* around  $\tilde{q} = -q_0$  and  $k_0^y = \pm\pi$ ,  $k_0^z = \pm\pi$ . The volume of the electron pocket is the same as the sum of the volumes of the hole pockets. When the pockets are very small their shape can be determined by expanding Eq.(42) around the point  $(\mathbf{0}, q_0)$ , using that

$$T_\perp(\mathbf{k}) \approx T_\perp(\mathbf{0})[1 - \mathbf{k}_\perp^2 \gamma^2].$$

Here  $\mathbf{k}_\perp$  denotes the deviation in the transverse direction from  $\mathbf{0}$  and  $\gamma$  is proportional to the lattice spacing in the transverse directions  $a_\perp$ . We obtain

$$2T_\perp^2(\mathbf{0})\gamma^2 \mathbf{k}_\perp^2 + \frac{b}{2}(q - q_0)^2 = T_\perp(\mathbf{0})^2 - (t_\perp^{\min})^2, \quad (46)$$

where

$$b = \frac{v_c^2}{Z_0^2} \frac{(x_0 + 1)(4\alpha x_0 - 3\alpha + 1)}{x_0(x_0 - 1)}.$$

We also can estimate the anisotropy of the Fermi surface from (46). The anisotropy of the masses is given by

$$\frac{m_\perp}{m_\parallel} = \frac{v_c^2}{4\gamma^2 m^2} \frac{(x_0 + 1)(4\alpha x_0 - 3\alpha + 1)}{x_0^3(1 + \alpha x_0)}, \quad (47)$$

where we have further approximated  $T_\perp(\mathbf{0}) \approx t_\perp^{\min}$ . Using that  $v_c \simeq 2ta_\parallel$ , where  $a_\parallel$  is the lattice spacing along the chains, we find that



$$\frac{m_{\perp}}{m_{\parallel}} \simeq \mathcal{A} \frac{a_{\parallel}^2}{\gamma^2} \frac{t^2}{m^2}, \quad (48)$$

where  $\mathcal{A}$  varies between 1.06 for  $v_s \rightarrow v_c$  and 0.62 for  $v_s \rightarrow 0$ . Thus the magnitude of the mass ratio is determined by the competition of two factors one of which is large ( $t/m$ ) and the other is small ( $a_{\parallel}/\gamma$ ). As a result, the Fermi surface may not be very anisotropic.

An obvious question is whether or not the RPA can be trusted to describe correctly the formation of a Fermi surface. An obvious problem of the RPA is that it automatically reproduces a purely one dimensional result at the particular wave numbers  $\mathbf{p}$  where the transverse hopping vanishes  $T_{\perp}(\mathbf{p}) = 0$ . On a 2D square lattice this would be at the points  $p_y = \pm\pi/2$ . In the case of coupled Luttinger liquids the improved treatment of<sup>11</sup> indicates that in the vicinity of these points RPA is unreliable. In the case of coupled Mott insulators, the electron and hole pockets we find for sufficiently large  $t_{\perp}$  are located at positions far away from the points where  $T_{\perp}(\mathbf{k})$  vanishes.

Recently a dynamical mean field theory approach has been developed, which replaces the quasi-1D system by a single effective chain, from which electrons can hop to a self-consistent bath<sup>27,28</sup>. The resulting model has to be analyzed by numerical methods and for coupled Hubbard chains it is found that for sufficiently large transverse hopping amplitudes an open Fermi surface (close to the one of the noninteracting model) is formed. This is in contrast to the electron and hole pockets we find in the RPA.

## VI. TRANSVERSE CONDUCTIVITY AND DENSITY OF STATES

Using the results for uncoupled chains as well as the RPA expression for the Green's function of weakly coupled chains we can determine various other physical quantities.

### A. The transverse conductivity

Let us consider a situation where the transverse hopping is only between nearest neighbour chains. The transverse current operator is then given by

$$j_{\perp}(x, l) = iet_{\perp} \left[ R_{\sigma}^{(l)}(x) R_{\sigma}^{(l+1)\dagger}(x) - \text{h.c.} + R \rightarrow L \right], \quad (49)$$

where  $l$  is a chain index and  $x$  denotes the position along the chain direction. Using this expression we can analytically determine the leading contribution in  $t_{\perp}$  to the transverse conductivity by using the result for the Green's function of uncoupled chains. We find

$$\sigma_{\perp}(\omega) = \frac{2Z_0^2 e^2 t_{\perp}^2}{\pi(v_c - v_s)} \frac{1}{\omega} \arctan \frac{4m\delta\sqrt{\omega^2 - 4m^2}}{\omega^2 + \delta(\omega^2 - 8m^2)}, \quad (50)$$

where  $\delta = (v_c - v_s)/(v_c + v_s)$ .

In the limit  $v_s \rightarrow v_c = v$  this simplifies to

$$\sigma_{\perp}(\omega) = \frac{2Z_0^2 e^2 t_{\perp}^2}{\pi v} \frac{1}{\omega} (2m/\omega)^2 \sqrt{(\omega/2m)^2 - 1} \quad (51)$$

We see that the transverse conductivity vanishes at the threshold  $\omega = 2m$  and increases above it in a characteristic square root fashion. This is reminiscent of the behaviour found for the longitudinal conductivity in<sup>39</sup>.

### B. Density of States

Within the RPA we can determine the density of states by integrating the RPA spectral function over all momenta. This needs to be done numerically. For simplicity we only consider the case  $v_c = v_s = v$ . For a 2D system with  $T_{\perp}(k_y) = t_{\perp} \cos(k_y)$ <sup>29</sup> we obtain the results shown in Fig.9. As  $t_{\perp}$  is increased, the Mott gap in the DOS is filled in and eventually a peak forms around zero energy.

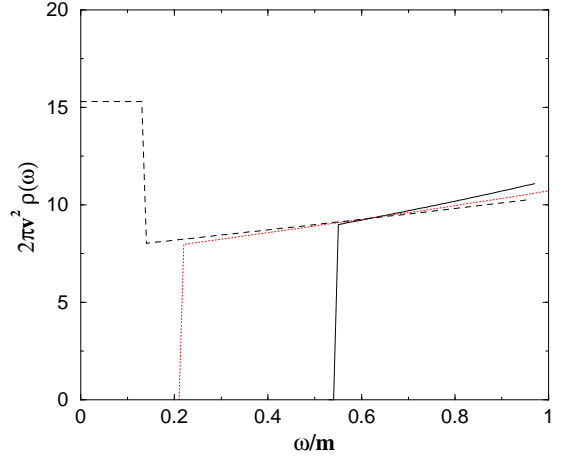


FIG. 9. Density of states for a 2D square lattice for frequencies smaller than the Mott gap. The curves are for  $t_{\perp} = 2$  (solid),  $t_{\perp} = 3$  (dotted) and  $t_{\perp} = 4$  (dashed).

The analogous analysis for a quasi 3D system with  $T_{\perp}(k_y, k_z) = t_{\perp} [\cos(k_y) + \cos(k_z)]$  yields a qualitatively different result. As  $t_{\perp}$  is increased the Mott gap is again filled in, but now the DOS around  $\omega = 0$  remains basically flat and no peak develops in the regime where RPA applies, i.e.  $t_{\perp}/m = \mathcal{O}(1)$ . In order to understand this result it is instructive to consider the case

$$T_{\perp}(\mathbf{k}) = t_{\perp} \sum_{j=1}^D \cos k_j, \quad D \gg 1. \quad (52)$$

In this limit  $T_{\perp}(\mathbf{k})$  can be considered to be a random variable with probability distribution

$$P(t) = \frac{1}{\sqrt{\pi D t_{\perp}^2}} \exp\left(-\frac{t^2}{D t_{\perp}^2}\right). \quad (53)$$

As we are interested in the formation of a Fermi surface we have to consider  $T_{\perp}(\mathbf{k}) = \mathcal{O}(m)$ , which implies that  $t_{\perp}D/m = \mathcal{O}(1)$ . This leads to the restriction that for large  $D$

$$t_{\perp} \propto \frac{m}{D}, \quad (54)$$

so that the probability distribution (53) becomes extremely narrow and only regions in  $k$ -space with  $T_{\perp}(\mathbf{k}) \approx 0$  contribute to the DOS. However, in these regions there are no states at  $\omega \approx 0$  and there will therefore be no peak in the DOS at low energies.

## VII. BECHGAARD SALTS AS A POSSIBLE APPLICATION

Our theory may be relevant to the Bechgaard salts and in particular to  $(\text{TMTTF})_2\text{PF}_6$  and  $(\text{TMTSF})_2\text{PF}_6$ . (see<sup>30, 31</sup> for a review). However, for our theory to be relevant, certain conditions must be met and this requires a discussion. The materials in question are quasi-one-dimensional and have a 3/4-filled band. The ratio of the hopping integrals in the three principal crystallographic directions is  $t_a : t_b : t_c = 1 : 0.1 : 0.005$ . Therefore, at sufficiently high temperatures one may neglect the hopping in the  $c$ -direction. Then one is left with a two-dimensional system of chains where each chain has only two nearest neighbours ( $\mathcal{N} = 2$ ). Such small number of nearest neighbours may put into question the applicability of RPA. This is, however, not the main worry.

The principal problem one encounters in dealing with the Bechgaard salts is the problem identifying the correct low-energy effective theory. Let us neglect the interchain hopping for the time being and consider uncoupled 1D chains. In the Bechgaard salts there are two separate mechanisms that have the potential to open a spectral gap. Firstly there are “double” Umklapp processes due to the commensurate band filling 3/4<sup>43,44</sup>. These processes involve the scattering of four electrons at  $k_F$  and four holes at  $-k_F$  and are generated in the low-energy effective theory by integrating out high energy modes. These processes will generate a gap only for strong interactions ( $K_c < 0.25$ ). Secondly there is a small dimerization, which halves the Brillouin zone and gives rise to “single” Umklapp processes<sup>45,46</sup>. These open a gap already for weak interactions  $K_c < 1$  but their coupling constant is proportional to the dimerization and thus small. At low energies the system is thus described by two independent Gaussian models - one for the charge and the other for the spin sector. The charge sector Gaussian model is perturbed by two operators: the  $4k_F$ -harmonics (with  $k_F$  being equal to  $3\pi/2a$ ) of the dimerization

$$\hat{D} = \delta t \sum_n (-1)^n c_{n+1,\sigma}^+ c_{n,\sigma} \quad (55)$$

where  $\delta t$  is a staggered component of the hopping integral, and the  $8k_F$  component of the electron density

operator (double-Umklapp processes). Since these operators have different symmetry under parity transformation (one is defined on links and the other on sites), in the continuous limit they are given by sin and cos respectively, such that the related Hamiltonian density is

$$V = g_1 \sin(\sqrt{8\pi K_c} \Phi_c) + g_2 \cos(2\sqrt{8\pi K_c} \Phi_c). \quad (56)$$

The behaviour of the system and applicability of our theory depend crucially on the value of  $K_c$ . We can consider the following possibilities.

(i) The interactions are weak and  $K_c \approx 1$ <sup>45,47</sup>. That the interactions are moderate is suggested by the renormalization of the uniform magnetic susceptibility with respect to the value extracted from the band structure calculations:  $\chi_s/\chi_0 \approx 2-3$ <sup>31</sup>. In this case, the  $g_2$ -term in (56) is irrelevant and the first term (due to dimerization) gives the sine-Gordon model which is equivalent to the charge sector of the Thirring model we have discussed. All our calculations are valid in this case.

If we adopt this scenario we have problems with Angle Resolved Photoemission (ARPES) data which do not show any traces of quasiparticles<sup>32,33</sup>. We will return to the question about ARPES data later.

(ii) There is a school of thought which advocates the small value  $K_c \approx 0.22$  when both operators are relevant<sup>34</sup>. According to this school, the dimerization coupling is small and the  $g_2$ -term dominates. This would agree qualitatively with ARPES data.

If this point of view is correct, the calculations presented in this paper are not applicable because, as it follows from<sup>15</sup>, for such values of  $K_c$  the minimal form-factor corresponds to the emission of not one, but two solitons. We have discussed this scenario in our other publication<sup>38</sup>. Here we cite just one conclusion from this paper: if  $K_c$  is small and the dimerization term is negligible, the value of the gap measured by ARPES should be equal to the optical gap observed in the frequency dependence of the on-chain conductivity, or twice the value of the activation gap in the temperature dependence of the dc conductivity:

$$\Delta_{\text{ARPES}} = 2E_{\text{act}} = \Delta_{\text{opt}} = 2m \quad (57)$$

Indeed, in  $(\text{TMTTF})_2\text{PF}_6$  ARPES measures a gap  $\Delta \approx 100$  meV and thermal conductivity measurements give the activation gap  $E_{\text{act}} = 44$  meV<sup>35</sup>, which is roughly one half.

(iii) The third possible scenario is that  $K_c$  is small, but the dimerization is not negligible. To resolve this issue theoretically one has to estimate the bare values of the coupling constants  $g_{1,2}$ . We know how to do this only for small  $U$ , where perturbation theory gives the following estimate

$$g_2 \sim E_0(U/E_0)^3.$$

If both terms are relevant and the sign of  $g_2$  is positive, as it follows from the perturbative calculation, then the

$g_1$ -term leads to the confinement of the solitons in the  $g_2$ -sine-Gordon model. This is a rather difficult case for the theory because the double sine-Gordon model is not integrable.

Let us assume for the time being that  $K_c \approx 1$  and see how our theory would square with experiment. (TMTTF) $_2$ PF $_6$  is a Mott insulator; the Fermi energy is estimated as 115 meV, the hopping integral in the  $b$ -direction is of order of 14 meV, the optical gap  $\Delta_{\text{opt}} = 2m$  is of order of 900K. Here the transverse tunneling is not large enough to overcome the Mott gap. In trying to get a detailed comparison with our calculations one has to take into account that the ratio  $m/\epsilon_F \approx 1/3$  is not very small here, which reduces the chances of obtaining a quantitative agreement with any field theoretical approach.

(TMTSF) $_2$ PF $_6$  is metallic; the Fermi energy is estimated as 220 meV, the hopping integral in the  $b$ -direction is of order of 20 meV, the optical gap  $\Delta_{\text{opt}} = 2m$  is of order of 250K. This gives  $T_{\perp}(0)/m \approx 4$  so that the criterion for having a small Fermi surface  $Z_0 T_{\perp}(0)/m > 3.3$  is satisfied here. Optical measurements for this material show a metallic Drude peak with a tiny amount of spectral weight (3 percent), separated by a gap from a very strong continuum. The metallic character of these compounds is due to the transverse hopping<sup>37,35</sup>. For frequencies not too close to the gap the observed form of the optical conductivity in the direction along the chains is well described by the sine-Gordon model<sup>39</sup>. This fact together with the observed smallness of the Drude weight indicate that (TMTSF) $_2$ PF $_6$  is a good candidate for application of the present theory.

An additional argument in favour of small pockets of Fermi liquid is that not all physical properties of (TMTSF) $_2$ PF $_6$  demonstrate the same degree of anisotropy. For example, the measured anisotropy of the plasma frequency for the Drude peaks is only of a factor of 2<sup>40</sup>. On the other hand, for the ratio of hopping integrals predicted by the band theory one should expect it to be of order of  $(m_{\perp}/m_{\parallel})^{1/2} \approx 10$ . This fact in combination with the smallness of the Drude weight indicates that the Fermi surface is small and not very anisotropic. On the other hand, many of the properties of these material (especially the magnetic ones) are typically one-dimensional (see<sup>31</sup> for review). Thus the overall picture is in reasonable agreement with the scenario we present.

The analysis of the Drude peak given in<sup>34</sup> indicates that the best fit can be obtained if one assumes frequency dependent effective mass and the scattering rates in the Drude formula:

$$\sigma(\omega) = \frac{\omega_p^2}{4\pi} \frac{1}{\Gamma_1(\omega) - i\omega[\frac{m^*(\omega)}{m_{\text{band}}}]},$$

$$\frac{m^*(\omega)}{m_{\text{band}}} = 1 + \frac{\lambda_0}{1 + \alpha^2 \omega^2},$$

$$\Gamma_1(\omega) = \Gamma_0 + \frac{\lambda_0 \alpha \omega^2}{1 + \alpha^2 \omega^2}. \quad (58)$$

This fit is rather suggestive because the frequency dependence is quadratic, like in Fermi liquid theory. This feature supports the point of view that the Drude peak comes from small pockets of Fermi liquid.

There are other quasi-one-dimensional systems for which ARPES measurements have been performed: the blue bronze K $_{0.3}$ MoO $_3$ , which is metallic<sup>41</sup>, and the Mott insulator Sr $_2$ CuO $_3$ . The latter material, however, is not a good testing ground for our theory since the ratio of the Mott-Hubbard gap to the bandwidth is too large. The largeness of the gap precludes a detailed comparison with the results obtained in this paper. On the qualitative side the measurements demonstrate the appearance of two distinct dispersing maxima in the spectral function<sup>42</sup>, which is interpreted as a sign of spin-charge separation.

ARPES is not the only way to ascertain the existence of quasi-particles. de Haas-van Alphen and Schubnikov-de Haas effects are perfect tools when one deals with closed Fermi surfaces. Obviously, the measurements should be made above the ordering temperature which may impose serious difficulties.

## ACKNOWLEDGMENTS

This work was started at the Isaac Newton Institute for Mathematical Sciences in Cambridge during the program on Strongly Correlated Electrons in 2000. We are grateful to the Institute for hospitality. Our warmest thanks are to Sergei Lukyanov for his help and interest to the work. We acknowledge illuminating conversations with A. Chubukov, N. D'Ambrumenil, A. Finkelstein, T. Giamarchi, A. Georges, V. Yakovenko and P. Wiegmann. We also thank S. Kivelson and D. Orgad for useful correspondence. This work was supported by the EPSRC under grants AF/100201 and GR/N19359 (FHLE) and by the DOE under contract number DE-AC02-98 CH 10886.

## APPENDIX A: ELEMENTS OF RPA

In this appendix we discuss some relevant aspects of the RPA in the interchain coupling. This is most easily done in position space. We denote the right and left-moving fermion operators by black and white circles. 1D correlation functions are denoted by encircling a number of circles, the corresponding fermion operators are then all located on the same chain. In Fig.10 we show the corresponding diagrams for the 1D two-point functions of right movers and left movers as well as the diagram from the 2n-point function of right movers. Finally, we denote the interchain hopping matrix element  $t_{ij}(x-y)$  between sites  $x/a_0$  on chain  $i$  and site  $y/a_0$  on chain  $j \neq i$  by a dashed line. We note that the hopping is local in time.

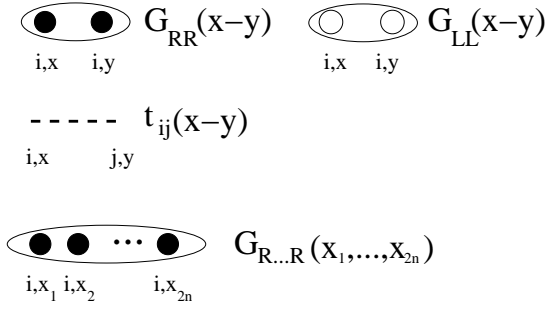


FIG. 10. Elements of the diagram technique in position space. Only one kind of many-particle “vertex” is shown.

The first few diagrams in the expansion (in the inter-chain hopping) of the two-point function of right moving electrons for initial and final point located on the same chain is shown in Fig.11. The contribution of a given diagram is obtained by summing over the positions of all “internal” circles, that is circles connected by a hopping line.

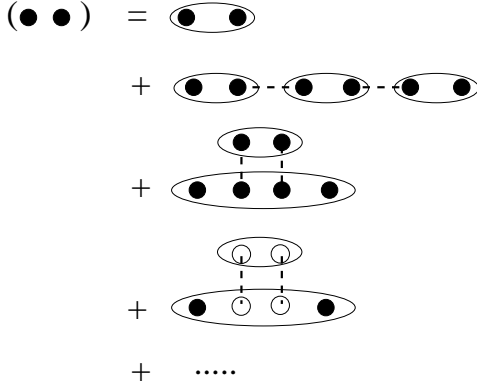


FIG. 11. Diagrams for initial and final points on the same chain up to second order in the interchain hopping.

The RPA expression for the (Fourier transform) of the single-particle Green’s function is obtained by summing all diagrams that can be split into two parts by cutting any one hopping line, i.e. all diagrams of the type shown in Fig.12.

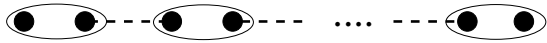


FIG. 12. Diagrams entering the RPA expression for the single-particle Green’s function. The sum is over all diagrams of the type shown.

All diagrams neglected in RPA all contain loops. This enables us to embed RPA into a systematic perturbative expansion in a small parameter  $\kappa_0$  as follows. Let us consider an interchain hopping  $T_\perp(\mathbf{k})$  (for simplicity we take it independent of the wave number  $q$  along the chain direction) of the form shown in Fig.13 i.e. particle-hole symmetric but long ranged such that its Fourier transform is strongly peaked around the origin and the point

$(0, \pi, \pi)$ . This means that in position space the hopping is *long-ranged*, i.e. the hopping amplitudes are of the same order within a range proportional to  $\kappa_0^{-1}$ .

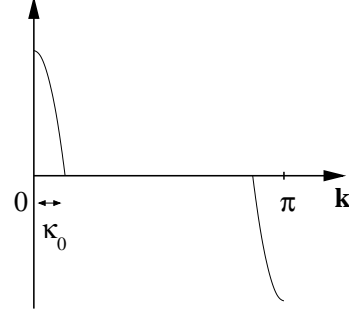


FIG. 13. Schematic dependence of  $T_\perp(\mathbf{k})$  on the transverse momenta  $q_\perp$ .

Every loop gives a contribution

$$\frac{1}{V} \sum_{\mathbf{k}} [T_\perp(\mathbf{k})]^2 \propto \kappa_0^2 \quad (\text{A1})$$

and is thus suppressed. In this way one obtains a formal expansion in powers of  $\kappa_0^2$ , the leading ( $\kappa_0^0$ ) order of which is given by the RPA.

## APPENDIX B: FORMFACTOR APPROACH IN INTEGRABLE QUANTUM FIELD THEORIES

The spectrum of low-lying excitations of the half-filled Hubbard model consists of scattering states of gapped, spinless charge  $\pm e$  excitations called *holons* and *antiholons* and gapless, charge-neutral excitations carrying spin  $\pm \frac{1}{2}$ , the so-called *spinons*<sup>48</sup>. We introduce labels  $h, \bar{h}, s, \bar{s}$  to distinguish between these four types of elementary excitations. Their dispersions and exact scattering matrices are known on the lattice<sup>48</sup> as well as in the field theory limit<sup>49</sup>. As usual for particles with relativistic dispersion it is useful to introduce rapidity variables  $\theta_{c,s}$  to parametrize energy and momentum

$$\begin{aligned} E_\alpha(\theta_c) &= m \cosh \theta_c, \quad P_\alpha(\theta_c) = m \sinh \theta_c, \quad \alpha = h, \bar{h}, \\ E_\gamma(\theta_s) &= \frac{m}{2} e^{\pm \theta_s}, \quad P_\gamma(\theta_s) = \pm \frac{m}{2} e^{\pm \theta_s}, \quad \gamma = s, \bar{s}. \end{aligned} \quad (\text{B1})$$

Here we have set spin and charge velocities to 1. Let us now turn to the construction of a basis of scattering states of holons, antiholons and spinons. A convenient formalism to this end is obtained in terms of the Zamolodchikov-Faddeev (ZF) algebra. The ZF algebra can be considered to be the extension of the algebra of creation and annihilation operators for free fermion or bosons to the case of interacting particles with factorizable scattering. The ZF algebra is based on the knowledge of the exact spectrum and scattering matrix<sup>48</sup>. For the SGM the ZF operators (and their hermitian conjugates) satisfy the following algebra

$$\begin{aligned}
Z^{\epsilon_1}(\theta_1)Z^{\epsilon_2}(\theta_2) &= S_{\epsilon'_1, \epsilon'_2}^{\epsilon_1, \epsilon_2}(\theta_1 - \theta_2)Z^{\epsilon'_2}(\theta_2)Z^{\epsilon'_1}(\theta_1), \\
Z_{\epsilon_1}^\dagger(\theta_1)Z_{\epsilon_2}^\dagger(\theta_2) &= Z_{\epsilon'_2}^\dagger(\theta_2)Z_{\epsilon'_1}^\dagger(\theta_1)S_{\epsilon_1, \epsilon_2}^{\epsilon'_1, \epsilon'_2}(\theta_1 - \theta_2), \\
Z^{\epsilon_1}(\theta_1)Z_{\epsilon_2}^\dagger(\theta_2) &= Z_{\epsilon'_2}^\dagger(\theta_2)S_{\epsilon_2, \epsilon'_1}^{\epsilon'_2, \epsilon_1}(\theta_2 - \theta_1)Z^{\epsilon'_1}(\theta_1) \\
&\quad + (2\pi)\delta_{\epsilon_2}^{\epsilon_1}\delta(\theta_1 - \theta_2). \tag{B2}
\end{aligned}$$

Here  $S_{\epsilon'_1, \epsilon'_2}^{\epsilon_1, \epsilon_2}(\theta)$  are the (factorizable) two-particle scattering matrices and  $\varepsilon_j = s, \bar{s}, h, \bar{h}$ .

Using the ZF generators a Fock space of states can be constructed as follows. The vacuum is defined by

$$Z_{\varepsilon_i}(\theta)|0\rangle = 0. \tag{B3}$$

Multiparticle states are then obtained by acting with strings of creation operators  $Z_\epsilon^\dagger(\theta)$  on the vacuum

$$|\theta_n \dots \theta_1\rangle_{\epsilon_n \dots \epsilon_1} = Z_{\epsilon_n}^\dagger(\theta_n) \dots Z_{\epsilon_1}^\dagger(\theta_1)|0\rangle. \tag{B4}$$

In term of this basis the resolution of the identity is given by

$$\sum_{n=0}^{\infty} \sum_{\epsilon_i} \int_{-\infty}^{\infty} \frac{d\theta_1 \dots d\theta_n}{(2\pi)^n n!} |\theta_n \dots \theta_1\rangle_{\epsilon_n \dots \epsilon_1} {}^{\epsilon_1 \dots \epsilon_n} \langle \theta_1 \dots \theta_n|. \tag{B5}$$

Inserting (B5) between operators in a 2-point function we obtain the following spectral representation

$$\begin{aligned}
\langle \mathcal{O}(x, t) \mathcal{O}^\dagger(0, 0) \rangle &= \sum_{n=0}^{\infty} \sum_{\epsilon_i} \int \frac{d\theta_1 \dots d\theta_n}{(2\pi)^n n!} \\
&\times \exp\left(i \sum_{j=1}^n P_{\epsilon_j}(\theta_j)x - E_{\epsilon_j}(\theta_j)t\right) \\
&\times |\langle 0 | \mathcal{O}(0, 0) | \theta_n \dots \theta_1 \rangle_{\epsilon_n \dots \epsilon_1}|^2, \tag{B6}
\end{aligned}$$

where

$$f^{\mathcal{O}}(\theta_1 \dots \theta_n)_{\epsilon_1 \dots \epsilon_n} \equiv \langle 0 | \mathcal{O}(0, 0) | \theta_n \dots \theta_1 \rangle_{\epsilon_n \dots \epsilon_1} \tag{B7}$$

are the form factors.

- 
- <sup>1</sup> N. F. Mott, *Metal-Insulator Transitions*, 2<sup>nd</sup> ed., Taylor and Francis, London (1990); F. Gebhard, *The Mott Metal-Insulator Transition*, Springer, Berlin (1997).  
<sup>2</sup> N. F. Mott, Proc. Roy. Soc. A**62**, 416 (1949); Canad. Jo. Phys. **34**, 1356 (1964); Phil. Mag. **6**, 287 (1961).  
<sup>3</sup> J. Hubbard, Proc. Roy. Soc. A**284**, 401 (1964).  
<sup>4</sup> L. B. Ioffe and A. I. Larkin, Phys. Rev. B**39**, 8988 (1989).  
<sup>5</sup> G. Kotliar and J. Liu, Phys. Rev. Lett. **15**, 1784 (1988); M. Grilli and G. Kotliar, Phys. Rev. Lett. **64**, 1170 (1990).  
<sup>6</sup> A. Georges, G. Kotliar, W. Krauth and M.J. Rozenberg, Rev. Mod. Phys. **68**, 13 (1996).

- <sup>7</sup> W. Metzner and D. Vollhardt, Phys. Rev. Lett. **62**, 324 (1989),  
D. Vollhardt, Int. Jour. Mod. Phys. **B3**, 2189 (1989).  
<sup>8</sup> R.M. Noack and F. Gebhard, Phys. Rev. Lett. **82**, 1915 (1999).  
<sup>9</sup> X.G. Wen, Phys. Rev. B**42**, 6623 (1990).  
<sup>10</sup> D. Boies, C. Bourbonnais and A.-M. S. Tremblay, Phys. Rev. Lett. **74**, 968 (1995).  
<sup>11</sup> E. Arrigoni, Phys. Rev. B**61**, 7909 (2000).  
<sup>12</sup> E. Jeckelmann, F. Gebhard and F. H. L. Essler, Phys. Rev. Lett. **85**, 3910 (2000).  
<sup>13</sup> *Bosonization and Strongly Correlated Systems*  
A. O. Gogolin, A. A. Nersisyan and A. M. Tsvelik, Cambridge University Press (1999).  
<sup>14</sup> F. A. Smirnov, *Form Factors in Completely Integrable Models of Quantum Field Theory*, World Scientific, Singapore (1992),  
M. Karowski and P. Weisz, Nucl. Phys. **B139**, 455 (1978),  
H. Babujian, A. Fring, M. Karowski and A. Zapletal, Nucl. Phys. **B538**, 535 (1999),  
A. Fring, G. Mussardo and P. Simonetti, Nucl. Phys. **B393**, 413 (1993).  
<sup>15</sup> S. Lukyanov and A. B. Zamolodchikov, preprint hep-th/0102079.  
<sup>16</sup> G. Delfino and G. Mussardo, Nucl. Phys. **B455**, 724 (1995).  
<sup>17</sup> P. B. Wiegmann, Sov. Sci. Rev. Ser. A, vol.2, p.41 (1980), Harwood Academic Publ., ed. I. M. Khalatnikov.  
<sup>18</sup> J. Voit, Eur. Phys. J. **B5**, 505 (1998).  
<sup>19</sup> O.A. Starykh, D.L. Maslov, W. Husler, L.I. Glazman, in *Low-Dimensional Systems*, ed. T. Brandes, Lecture Notes in Physics, Springer (2000).  
<sup>20</sup> D. Orgad, Philos. Mag. **B81**, 377 (2001).  
<sup>21</sup> A. Parola and S. Sorella, Phys. Rev. B **45**, 13156 (1992), Phys. Rev. B **57**, 6444 (1998).  
<sup>22</sup> M.B. Halpern, Phys. Rev. **D12**, 1684 (1976),  
R. Köberle, V. Kurak and J.A. Swieca, Phys. Rev. **D20**, 897 (1979).  
<sup>23</sup> B. A. Bernevig, D. Guiliano and R. B. Laughlin, preprint cond-mat-0105523.  
<sup>24</sup> V. Meden and K. Schönhammer, Phys. Rev. B**46**, 15753 (1992).  
<sup>25</sup> P.W. Anderson, Phys. Rev. Lett. **67**, 3844 (1991).  
<sup>26</sup> I.E. Dzyaloshinskii, unpublished.  
<sup>27</sup> A. Georges, T. Giamarchi and N. Sandler, Phys. Rev. **B61**, 16393 (2000).  
<sup>28</sup> S. Biermann, T. Giamarchi, A. Georges and A. Lichtenstein, preprint cond-mat/0107633.  
<sup>29</sup> Here we consider transverse hopping between n.n. chains, so that RPA is not a controlled approximation.  
<sup>30</sup> T. Ishiguro and K. Yamji, *Organic Superconductors*, Springer Verlag, Berlin 1990.  
<sup>31</sup> C. Bourbonnais and D. Jerome, in “Advances in Synthetic Metals, Twenty years of Progress in Science and Technology”, ed. by P. Bernier, S. Lefrant and G. Bidan (Elsevier, New York, 1999), p. 206-301 and references therein. See also cond-mat - 9903101.  
<sup>32</sup> F. Zwick, S. Brown, G. Margaritondo, C. Merlic, M. Onellion, J. Voit and M. Grioni, Phys. Rev. Lett. **79**, 3982 (1997).  
<sup>33</sup> T. Valla and P. Johnson, unpublished.

- <sup>34</sup> A. Schwartz, M. Dressel, G. Grüner, V. Vescoli, L. Degiorgi, T. Giamarchi, Phys. Rev. B **58**, 1261 (1998),  
V. Vescoli, L. Degiorgi, W. Henderson, G. Grüner, K. P. Starkey, L. K. Montgomerly, *Science* **281**, 1181 (1998).
- <sup>35</sup> V. Vescoli *et al.* Science **281**, 1191 (1998).
- <sup>36</sup> M. Fabrizio, A. O. Gogolin and A. A. Nersesyan, Phys. Rev. Lett. **83**, 2014 (1999); Nucl. Phys. B **580**, 647 (2000).
- <sup>37</sup> T. Giamarchi, Physica B **230-232**, 975 (1997).
- <sup>38</sup> F. H. L. Essler and A. M. Tsvelik, preprint [cond-mat/0105582](#).
- <sup>39</sup> D. Controzzi, F. H. L. Essler and A. M. Tsvelik, Phys. Rev. Lett. **86**, 960 (2001).
- <sup>40</sup> W. Henderson, V. Vescoli, P. Tran, L. Degiorgi and G. Grüner, Eur. Phys. J. B **11**, 365 (1999).
- <sup>41</sup> G.H. Gweon, J.W. Allen et.al., J. Phys. Cond. Mat. **8**, 9923 (1996).
- <sup>42</sup> C. Kim, Z.X. Shen, N. Montoyama, H. Eisaki, S. Uchida, T. Tohyama and S. Maekawa, Phys. Rev. B **56**, 15589 (1997).
- <sup>43</sup> T. Giamarchi, Physica B **230-232**, 975 (1997).
- <sup>44</sup> H. Yoshioka, M. Tsuchizu and Y. Suzumura, J. Phys. Soc. Jpn **70**, 762 (2001).
- <sup>45</sup> V.J. Emery, R. Bruinsma and S. Barisic, Phys. Rev. Lett. **48**, 1039 (1982).
- <sup>46</sup> K. Penc and F. Mila, Phys. Rev. B **50**, 11429 (1994).
- <sup>47</sup> S. Brazovskii and V. Yakovenko, Sov. Phys. JETP **62**, 1340 (1985).
- <sup>48</sup> F.H.L. Essler and V.E. Korepin, Phys. Rev. Lett. **72**, 908 (1994); Nucl. Phys. B **426**, 505 (1994).
- <sup>49</sup> E. Melzer, Nucl. Phys. B **443**, 553 (1995).